Published as *Physical Review A* **85**, 062503 (2012) on 5 June 2012

Linear quantum capacitance scaling for lanthanide and actinide atoms: analysis of two differing sets of electron affinity predictions

William E. Bunting and James C. Ellenbogen*
Nanosystems Group, The MITRE Corporation, McLean, Virginia 22101, USA

(Dated: May 28, 2012)

Scaling of quantum capacitances is explored for lanthanide and actinide atoms. For lighter atoms, quantum capacitances have been seen to scale linearly with mean radii of the atoms' outermost occupied orbitals. This scaling law is used to analyze two recent, differing sets of theoretical calculations for lanthanide electron affinities A. Consistent with the scaling law, A values predicted by O'Malley and Beck for lanthanides [*Phys. Rev. A*, **78**, 012510 (2008)], using a relativistic configuration interaction (RCI) method, produce capacitances that scale with the atoms' mean radii along a single line to a high degree of confidence. Similar linear scaling behavior also results for the actinides from O'Malley's and Beck's RCI calculations of their A values. However, lanthanide A values predicted by Felfli *et al.* [*Phys. Rev. A*, **81**, 042707 (2010)], using a Regge-pole approach, unexpectedly produce capacitance scaling along two different lines for atoms with similar neutral electron configurations. Both types of linear capacitance scaling are internally consistent, though, and do not serve to determine definitively which set of electron affinity predictions for the lanthanides is likely to be more accurate. Still, evidence from this and prior capacitance scaling investigations tends to favor the O'Malley and Beck results. In addition, linear capacitance scaling for the actinides is applied to estimate the previously unknown A values for Fm and Md as 0.007 eV and -0.006 eV, respectively.

PACS numbers: 31.10.+z, 31.15.-p, 32.10.Hq, 31.90.+s

I. INTRODUCTION

Recently, there has been discussion in the literature about two new sets of values that have been predicted via theory for the electron affinities A of the lanthanide elements [1–4]. In addition, there have been new theoretical predictions of A values for the actinide elements [5]. In this paper, we use these new values to explore the scaling of quantum capacitances for lanthanide and actinide atoms as a function of mean radii for their outermost occupied orbitals. In the process, we analyze from a capacitance-based perspective, across the entire row of the perodic table, the two differing sets of predictions [1, 4] for the electron affinities of lanthanide atoms.

To do so, we apply the previously established law or principle [6–8] that quantum capacitances [9, 10]

$$C = 1/(I - A) \tag{1}$$

of atoms and molecules with similar neutral electron configurations scale linearly with the species' effective radii. For that purpose, we also use established values [11–13] of the atoms' valence ionization potentials I and mean radii $\langle r\rangle_a$.

We find that lanthanide A values from recent, detailed relativistic configuration interaction calculations by O'Malley and Beck [1] yield C values that scale with $\langle r\rangle_a$ in a strongly linear manner along a single line for all nine lanthanide atoms having N-electron, neutral electron configurations [Xe]$4f^n6s^2$, where $n \neq 7, 14$. This is seen in Fig. 1. By contrast, in Fig. 2, it is seen that the lanthanide A values calculated by Felfli *et al.* [4] for the same atoms, using a Regge pole method [3, 14], lead to capacitances that scale linearly with atomic mean radius in a more complex manner, along *two* lines, which are distinguished by properties of the $(N{+}1)$-electron states.

For the actinide atoms, we employ a similar approach, along with O'Malley and Beck's recent calculations [5] of their A values, to show that linear capacitance scaling applies for the actinides, as well. See Fig. 3. Then, we use the linear scaling equation and known values of I and $\langle r\rangle_a$ to provide approximate values of A for two actinide atoms, Fm and Md, for which no values were known.

II. METHOD AND RESULTS

Figures 1 and 2 plot C versus $\langle r\rangle_a$ for the lanthanide atoms using values presented in Table I. For Fig. 1, values of C are those from column 8 of the table and are derived via Eq. (1) from lanthanide A values in column 6, calculated by O'Malley and Beck [1, 2]. On the other hand, Fig. 2 uses C values from column 9, as derived from A values of Felfli *et al.* [3] in column 7 of the table.

The plots in the figures are analogous to those presented in prior capacitance scaling analysis for lighter atoms [6], except that here it is necessary to account for relativistic effects on the dimensions of heavy atoms by using values of $\langle r\rangle_a$ from the Dirac-Fock calculations of Desclaux [13]. Throughout this work, the values of I and the ground-state electron configurations are from online tables provided by the National Institute of Standards and Technology (NIST) [11, 12]. Since I and A are given in units of eV, values of C calculated via Eq. (1) are in the atomic-scale units of fundamental positive charges per V

---

* ellenbgn@mitre.org

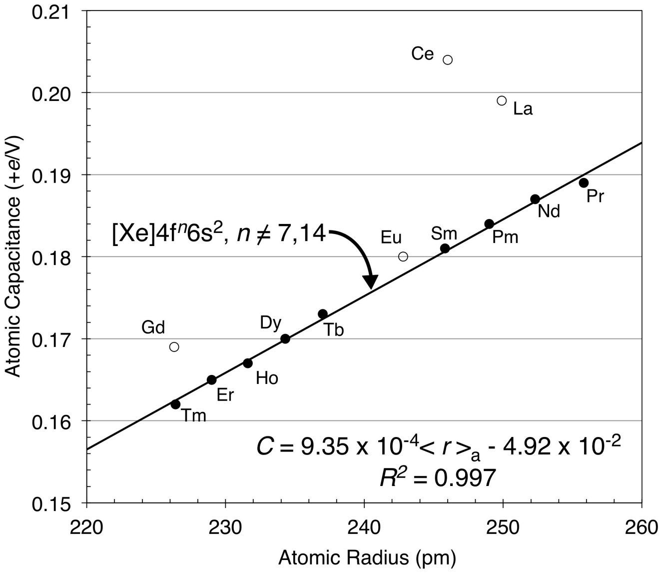

FIG. 1. O'Malley and Beck's A values for lanthanide atoms [1, 2] are used to calculate their quantum capacitances in fundamental positive charges per volt ($+e$/V), which are plotted here versus the atoms' mean radii. Coordinates of the points are given in columns 4 and 8 of Table I. A regression line is fit to just the points plotted as dark filled circles, and parameters for the line are displayed in its regression equation and correlation coefficient. Filled and unfilled circles indicate different types of neutral electron configurations for the atoms the points represent. See text.

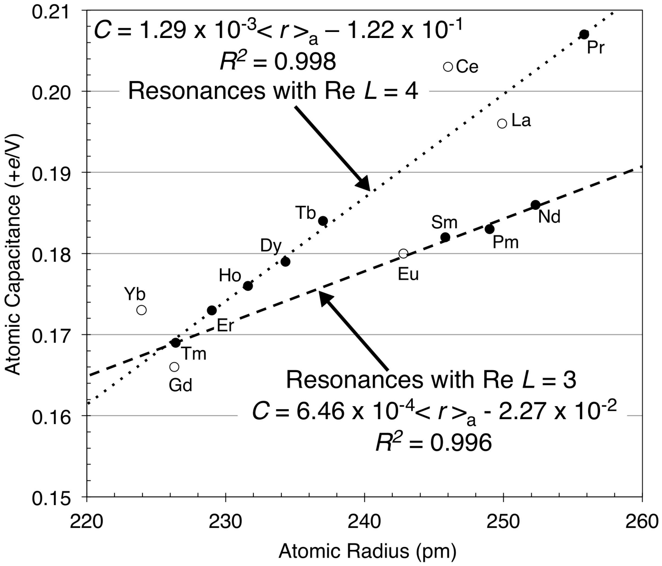

FIG. 2. Felfli *et al.*'s A values for lanthanide atoms [4] are used to calculate their quantum capacitances in fundamental positive charges per volt ($+e$/V), which are plotted here versus the atoms' mean radii. Coordinates of the points are given in columns 4 and 9 of Table I. Dotted and dashed regression lines each are fit to a different subset of the nine filled points, but intersect near the Tm point. Black-filled points correspond to neutral lanthanides with the electron configuration $[\mathrm{Xe}]4f^n6s^2$, $n \neq 7, 14$, while unfilled points correspond to other types of neutral electron configurations. For each line, the regression equation and correlation coefficient are displayed. Values of A for points along the dotted line are found here to correspond to anionic Regge resonances of Felfli *et al.* with $\mathrm{Re}\, L = 4$ for the real part of their complex total angular momentum; points along the dashed line correspond to $\mathrm{Re}\, L = 3$. See Table I and text.

(symbolized as "$+e$/V") [6], which we employ in the figures, tables, and text. Using these fundamental units of capacitance, from the graphs in Figs. 1, 2, and 3 it can be seen immediately that a lanthanide or actinide atom (i.e., an "atomic capacitor") sustains only a fraction of a fundamental positive charge under a potential of 1 V.

As in prior analyses of quantum capacitance scaling [6–8], scaling trends for the lanthanides and actinides are found to be very sensitive to the electron configurations of the atoms' neutral states. For example, while it is seen in Fig. 1 that the majority of radius-capacitance points obtained from O'Malley and Beck A values scale on a line (dark filled points), some points scale off the line (open unfilled points). We observe that all the dark points on this line (which we term "f-scaling points") represent atoms with neutral valence electron configurations that contain a partly filled f shell, but not one that is half or completely filled–i.e., f^n, $n \neq 7, 14$. Points that lie off the f-scaling line represent atoms with valence configurations that contain a d orbital, a half-filled f shell (i.e., f^7), or a completely filled f shell (i.e., f^{14}).

The f-scaling points and line in Fig. 1 appear to be analogous to the points and strong scaling line for the first and second row P-states in our analysis [6] of capacitance scaling for lighter atoms. As in that case, where just p orbitals are filled in the valence shells of the neutral atoms as one progresses across the row of the periodic table, when electrons are added to f orbitals to make successive neutral lanthanides, their radius-capacitance points scale along the same line (even though the points correspond to neutral configurations with different term symbols). Also, differently behaving points (open circles in the graphs) that correspond to atoms with half-filled or completely filled f-shells, and lie off the f-scaling line, are somewhat analogous to points for lighter atoms with half-filled p-shells (e.g., N, P, As) or completely filled p-shells (Ne, Ar, Kr), which lie off the P-state scaling line.

Regression analysis considering only the dark filled points is used to determine the lines in the plots for which equations of the form

$$C = B\langle r\rangle_a + C_0, \tag{2}$$

as well as correlation coefficients R^2, are displayed in Figs. 1 and 2. Per our comments in the Introduction, A values calculated by O'Malley and Beck for the nine dark filled radius-capacitance points that correspond to atoms with neutral electron configurations $[\mathrm{Xe}]4f^n6s^2$ are seen in Fig. 1 to yield a regression line with a very high correlation coefficient, R^2=0.997.

TABLE I. Atomic capacitances C for lanthanide atoms are calculated via Eq. (1) in fundamental positive charges per volt[a] and tabulated as a function of atomic mean radius $\langle r \rangle_a$, for two different sets of values predicted for the atoms' electron affinities A by O'Malley and Beck (O&B) [1] and by Felfli *et al.* [4], except as noted. Lanthanide experimental ionization potentials I are obtained from the *NIST Chemistry WebBook* [11], except for Pm. Values of $\langle r \rangle_a$ are from neutral ground-state (g.s.) relativistic Dirac-Fock calculations of Desclaux [13]. The real part of angular momentum Re L characterizes Regge resonances in calculation of A by Felfli *et al.* [4].

					A		C		
Atom	Atomic No., Z	Neutral g.s. Electron Configuration[d]	$\langle r \rangle_a$ (pm)	I (eV)	O&B (eV)	Felfli *et al.* (eV)	O&B (+e/V)	Felfli *et al.* (+e/V)	Re L
La	57	[Xe]$5d6s^2$	249.9	5.577	0.545[b]	0.480	0.199	0.196	4
Ce	58	[Xe]$4f5d6s^2$	246.0	5.539	0.628[c]	0.610	0.204	0.203	4
Pr	59	[Xe]$4f^36s^2$	255.8	5.464	0.177	0.631	0.189	0.207	4
Nd	60	[Xe]$4f^46s^2$	252.3	5.525	0.167	0.162	0.187	0.186	3
Pm	61	[Xe]$4f^56s^2$	249.0	5.582[d]	0.154	0.129	0.184	0.183	3
Sm	62	[Xe]$4f^66s^2$	245.8	5.644	0.130	0.162	0.181	0.182	3
Eu	63	[Xe]$4f^76s^2$	242.8	5.670	0.117	0.116	0.180	0.180	3
Gd	64	[Xe]$4f^75d6s^2$	226.3	6.150	0.234[b]	0.137	0.169	0.166	3
Tb	65	[Xe]$4f^96s^2$	237.0	5.864	0.085	0.436	0.173	0.184	4
Dy	66	[Xe]$4f^{10}6s^2$	234.3	5.939	0.063	0.350	0.170	0.179	4
Ho	67	[Xe]$4f^{11}6s^2$	231.6	6.022	0.050	0.338	0.167	0.176	4
Er	68	[Xe]$4f^{12}6s^2$	229.0	6.108	0.038	0.312	0.165	0.173	4
Tm	69	[Xe]$4f^{13}6s^2$	226.4	6.184	0.022	0.274	0.162	0.169	4
Yb	70	[Xe]$4f^{14}6s^2$	223.9	6.254	-	0.482	-	0.173	4
Lu	71	[Xe]$4f^{14}5d6s^2$	206.5	5.426	0.353[b]	0.415	0.197	0.200	4

[a] Columns marked +e/V report atomic capacitances in fundamental units of positive charge per volt. Multiplication by 1.602176×10^{-19} coulombs per fundamental unit of charge converts these capacitances to the more familiar mks units of farads. Using these capacitance units, the permittivity of free space is $\epsilon_0 = 5.526350 \times 10^{-5}$ +e/V-pm.

[b] Value of A from Ref. [2].

[c] Value of A from Ref. [15].

[d] From Ref. [12].

While the Felfli *et al.* points for those nine lanthanide atoms are not fit well by a single regression line, in Fig. 2 it is seen that two subsets of those points are fit very well by two intersecting regression lines. These are the dotted and dashed lines in Fig. 2. The Tm point, which lies very near the intersection of the two lines, is included only in the regression that produces the upper, dotted line in the graph. As is indicated on the graph, the points that determine these two different lines correspond to different values of the parameter Re L. (See Table I.) The quantity Re L is the real part of the complex total angular momentum L for the $(N+1)$-electron Regge resonances that Felfli et al. calculate and associate [3, 4, 14] with the ground anionic states of lanthanide atoms in order to determine their A values.

Now, considering the actinide atoms, we likewise derive quantum capacitances from values of A calculated by O'Malley and Beck [5]. These are presented in Table II and plotted versus $\langle r \rangle_a$ in Fig. 3. The four points in Fig. 3 displayed as black diamonds represent actinide f-scaling atoms with their outermost occupied orbitals in f shells that are partly filled, but not half filled. Much like the lanthanide case displayed in Fig. 1, regression analysis of these actinide points that represent similar neutral electron configurations yields a straight line with a very large correlation coefficient, $R^2 = 0.996$.

As part of the above-described method, for both lanthanide and actinide atoms we chose to use values of $\langle r \rangle_a$ from the Dirac-Fock calculations of Desclaux [13], in preference to those from the more recent work of Visscher and Dyall [16]. This is because, unlike the work of Desclaux, the Visscher and Dyall calculations for a number of the heavy atoms employ ground state atomic electron configurations that differ from those in the NIST tables [11, 12] where we obtain our experimental ionization potentials. For those atoms, the $\langle r \rangle_a$ values of Visscher and Dyall differ somewhat from the ones given by Desclaux, but all of those atoms have radius-capacitance points that fall off the scaling lines using mean radii from either source. In the cases of atoms that do have points on the scaling lines in Figs. 1, 2, and 3, the values of $\langle r \rangle_a$ obtained from Desclaux are the same, within a tenth of a pm, as those from all of the several types of finite-nucleus Dirac-Fock calculations performed in the work of Visscher and Dyall. Hence, the choice of the source for the radii does not substantively affect the scaling results presented here.

III. ANALYSIS AND PREDICTIONS

As in classical electrostatics, the scaling of the capacitances for neutral atomic and molecular-scale conductors is expected be determined by their shape and the dielectric constant of the surrounding medium. For lighter atoms [6] and for diatomic molecules [8], the effec-

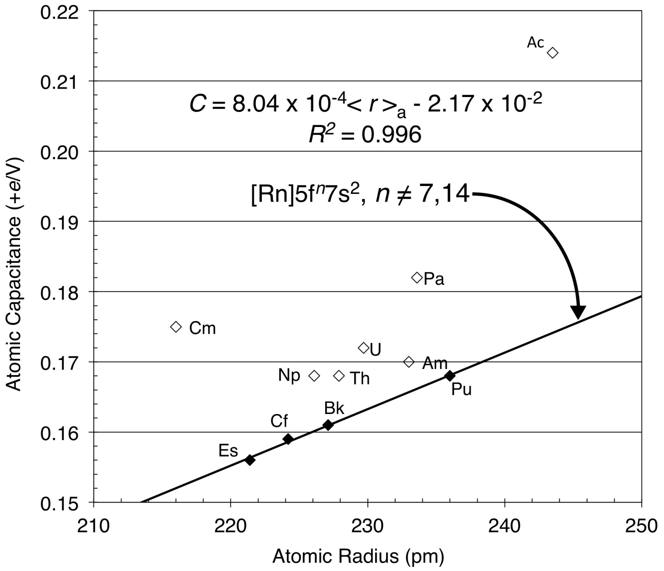

FIG. 3. O'Malley and Beck's A values for actinide atoms [5] are used to calculate their quantum capacitances in fundamental positive charges per volt ($+e$/V), which are plotted here versus the atoms' mean radii. Coordinates of the points are given in columns 4 and 7 of Table II. A regression line is fit to just the dark filled diamonds and parameters for the line are displayed in its regression equation. Filled and unfilled diamonds indicate different types of electron configurations for the atoms the points represent. See text.

TABLE II. Atomic capacitances C for the actinide atoms in fundamental positive charges per volt[a] are tabulated as a function of atomic mean radius $\langle r\rangle_a$. Capacitances are evaluated via Eq. (1) using electron affinities A calculated by O'Malley and Beck [5] and experimental ionization potentials I from the *NIST Chemistry WebBook* [11], except as noted. Values of $\langle r\rangle_a$ are from the ground-state (g.s.) relativistic Dirac-Fock calculations of Desclaux [13].

Name	Z	g.s. Electron Configuration[b]	$\langle r\rangle_a$ (pm)	I (eV)	A (eV)	C ($+e$/V)
Ac	89	[Rn]$6d7s^2$	243.5	5.170	0.491	0.214
Th	90	[Rn]$6d^27s^2$	227.9	6.307	0.368	0.168
Pa	91	[Rn]$5f^26d7s^2$	233.6	5.890	0.384	0.182
U	92	[Rn]$5f^36d7s^2$	229.7	6.194	0.373	0.172
Np	93	[Rn]$5f^46d7s^2$	226.1	6.266	0.313	0.168
Pu	94	[Rn]$5f^67s^2$	236.0	6.026	0.085	0.168
Am	95	[Rn]$5f^77s^2$	233.0	5.974	0.076	0.170
Cm	96	[Rn]$5f^76d7s^2$	216.0	6.020	0.321	0.175
Bk	97	[Rn]$5f^97s^2$	227.1	6.230	0.031	0.161
Cf	98	[Rn]$5f^{10}7s^2$	224.2	6.300	0.018	0.159
Es	99	[Rn]$5f^{11}7s^2$	221.4	6.420	0.002	0.156
Fm	100	[Rn]$5f^{12}7s^2$	218.6	6.500	-	-
Md	101	[Rn]$5f^{13}7s^2$	215.9	6.580	-	-
No	102	[Rn]$5f^{14}7s^2$	213.2	6.650	-	-
Lr	103	[Rn]$5f^{14}7s^27p$	194.5	4.900[b]	0.465	0.225

[a] See footnote a of Table I.

[b] From Ref. [12].

tive "shape", dielectric constant, and capacitance scaling line were found to be governed by the neutral-state term symbol or electron configuration. Especially, atoms with the same type of neutral-state electron configuration had radius-capacitance points that scaled along the same line; atoms with different neutral-state electron configurations had points that scaled along different lines.

Likewise, since all nine f-scaling lanthanide atoms have similar neutral electron configurations, it was expected that they would scale along the same line, in the manner of the P-states of lighter atoms, for example. Such expected behavior is exhibited in Fig. 1 by the lanthanide quantum capacitances determined from electron affinities calculated [1, 2] by O'Malley and Beck.

By this reasoning, in Fig. 2, the unexpected scaling along two lines could indicate a mutual inconsistency among the capacitances and, therefore, among the component A values given by Felfli *et al.* [4] for the nine f-scaling lanthanide atoms. On the other hand, although it contradicts the concept that the "shape" of the neutral state should determine its capacitance scaling, using Eq. (1) one can make a numerical argument that different scaling lines also can result from different "shapes" or electron configurations for the *anions*. Then, the two different scalings seen in Fig. 2 may be interpreted as an indication that in the Felfli *et al.* lanthanide electron affinity calculations the electron attachments to the neutral states are occurring consistently, but in two different ways (e.g., in two different orbitals or with two different angular momentum couplings), leading to two different types of electron configurations for the anions.

This is unlike electron attachments in the O'Malley and Beck lanthanide electron affinity calculations. In those calculations the extra electron is added in a $6p$ orbital for all nine atoms on the scaling line in Fig. 1. If all those anion attachments did not occur in such a simple manner, in the same orbital, the resulting capacitance scaling might not occur on a single line. There is some independent evidence from experiments [17, 18] and from theory [19], however, that electron attachments to produce lanthanide anions in their ground states do take place in $6p$ orbitals. This argues further in favor of capacitance scaling along a single line, like that in Fig. 1.

In the work of Felfli *et al.*, though, it is not easily determined in which orbital the extra electron is added to those nine neutral lanthanide atoms. This is because the many-electron Regge-pole method they employ does not appear to predict the electron configuration of the anionic state. Thus, the source of the two scaling lines in that work is somewhat difficult to understand or interpret in terms of a model for the anion involving configurations of orbitals. The two scalings do appear to depend, however, on Felfli *et al.* having associated the most stable anions for the various lanthanide atoms with electron-scattering resonances that have two different values for the real parts of their total angular momenta, $\mathrm{Re}\,L = 3$ and $\mathrm{Re}\,L = 4$. If this were not the case, the capacitance scaling might not occur along two different lines for atoms having the same type of neutral electron configuration. In this connection, it is noteworthy that in earlier work on the lanthanides [3] the same authors associated some of the lanthanide anions with resonances having different values for $\mathrm{Re}\,L$ than they do in their later work [4]. As a result, they originally made different predictions for the A values of those elements, which they later changed.

Turning our analysis to the actinide atoms, we note that O'Malley and Beck [5] did not present values of A for some of the actinide atoms having partly filled f shells in their valence configurations. Specifically, no electron affinities were predicted for Fm and Md. Also, no values for these quantities appear elsewhere in the literature.

As in prior work [8] on diatomic molecules with unknown values of A, here we are able to use capacitance scaling to estimate values of A for Fm and Md. First, we assume that the radius-capacitance points for these two actinide atoms scale on the same line with the other four actinide atoms having similar electron configurations. This assumption seems to be very reasonable, since points for the corresponding two lanthanide atoms, Er and Tm, scale on the line with the other lanthanides in Fig 1. Second, we rearrange Eq. (1) and use Eq. (2) to eliminate C, in order to derive the equation [6, 8]:

$$A = I - \frac{1}{C} = I - \frac{1}{B\langle r\rangle_a + C_0}. \tag{3}$$

Lastly, we apply this result and the values of B and C_0 given in Fig. 3 to evaluate, approximately, the unknown electron affinities of Fm and Md from their known values of I and $\langle r\rangle_a$. (See Table II.) The results are 0.007 ± 0.070 eV for Fm and -0.006 ± 0.070 eV for Md.

The relatively large uncertainties in the values of A for Fm and Md are due to correspondingly large uncertainties in the I values listed for these atoms in the *NIST Chemistry Webbook* [11]. However, uncertainties listed in that same source are much smaller (≤ 0.025 eV) for the I values of the actinide atoms whose radius-capacitance points we used to determine the regression line in Fig. 3. These uncertainties in I produce maximum capacitance uncertainties in C of $\pm 0.001 + e$/V. Further, the lanthanide ionization potentials all have much smaller uncertainties than for the actinides, producing maximum uncertainties in C of $\pm 0.0003 + e$/V. Thus, the regression lines and parameters in Figs. 1, 2, and 3 are negligibly affected by uncertainties in I. Uncertainties in A are not given by O'Malley and Beck or by Felfli *et al.*

Finally, we observe that we may further expand Eq. (2) and, thereby, amplify comments above concerning scaling being dependent upon an atom's dielectric properties. The coefficient of $\langle r\rangle_a$ in Eq. (2) may be expanded as $B = 4\pi\epsilon_0\kappa$, where $\epsilon_0 = 5.526350 \times 10^{-5}$ $+e$/V-pm is the permittivity of free space and κ may be interpreted as the dielectric constant of the atom's electron distribution [6]. From B values in Figs. 1 and 3, κ is found to be 1.346 and 1.158 for f-scaling lanthanide and actinide atoms, respectively.

Thus, when it is determined via regression using *ab initio* electron affinity values from O'Malley and Beck [1, 5], Eq. (2) generalizes to heavy lanthanide and actinide atoms the linear scaling relation $C = C_{sphere} = 4\pi\epsilon_0\kappa\langle r\rangle_a + C_0$. This equation applies to spheres in classical electrostatics and, as mentioned above, also governs [6] quantum capacitances for lighter atoms.

IV. SUMMARY AND CONCLUSIONS

In summary, this paper has shown that lanthanide electron affinities calculated by O'Malley and Beck [1, 2] produce quantum capacitances that scale linearly on a single line with the atoms' mean radii, consistent with scaling in lighter atoms. However, the different lanthanide electron affinity values given by Felfli *et al.* [4] produce quantum capacitance scaling along two different lines for atoms with similar neutral electron configurations.

We conclude that both these types of scaling are possible, algebraically. Thus, analysis based on capacitance scaling alone does *not* serve to determine definitively which of the two different sets of lanthanide electron affinity predictions, those of O'Malley and Beck or those of Felfli *et al.*, are likely to be more accurate. Each set of A values leads to a different kind of internally consistent linear scaling for quantum capacitances of the lanthanides as functions of their atomic mean radii.

Still, based upon earlier capacitance scaling investigations, the authors tend to favor the lanthanide electron affinity predictions of O'Malley and Beck. Capacitances derived from them conform to the principle established in the case of the light elements [6], wherein the states or electron configurations of the neutral atoms determine the line along which their capacitances scale. Also, using the A values of O'Malley and Beck, capacitance scaling for f-filling lanthanide atoms follows the pattern observed in p-filling first and second row neutral atoms. Further, work by investigators [17–19] other than O'Malley and Beck favors the $6p$ electron attachments that occur in their lanthanide electron affinity calculations and that appear to be instrumental in producing the single capacitance scaling line seen in Fig. 1.

We also have shown here that there is linear capacitance scaling in the case of the actinide atoms. Then, we have applied the associated linear scaling relation to estimate previously unknown electron affinities for two such atoms, Fm and Md, as 0.007 eV and -0.006 eV, respectively.

ACKNOWLEDGMENTS

The authors gratefully acknowledge valuable conversations and comments on the manuscript by S. Das, K. Eisenbeiser, J. Klemic, and G. Lewis of the MITRE Nanosystems Group. We thank M. Taczak for suggesting the topic of this investigation. This research was funded by the MITRE Innovation Program.

---

[1] S. M. O'Malley and D. R. Beck, Phys. Rev. A **78**, 012510 (2008)

[2] S. M. O'Malley and D. R. Beck, Phys. Rev. A **79**, 012511 (2009)

[3] Z. Felfli, A. Z. Msezane, and D. Sokolovski, Phys. Rev. A **79**, 012714 (2009)

[4] Z. Felfli, A. Z. Msezane, and D. Sokolovski, Phys. Rev. A **81**, 042707 (2010)

[5] S. M. O'Malley and D. R. Beck, Phys. Rev. A **80**, 032514 (2009)

[6] J. C. Ellenbogen, Phys. Rev. A **74**, 034501 (2006)

[7] J. C. Ellenbogen, C. A. Picconatto and J. S. Burnim, Phys. Rev. A **75**, 042102 (2007)

[8] J. C. Ellenbogen, Phys. Rev. A **82**, 012508 (2010)

[9] G. J. Iafrate, K. Hess, J. B. Krieger, and M. Macucci, Phys. Rev. B **52**, 10737 (1995)

[10] J. P. Perdew, Phys. Rev. B **37**, 6175 (1988)

[11] P. J. Lindstrom and W. G. Mallard, eds., *NIST Chemistry WebBook*, NIST Standard Reference Database No. 69 (Natl. Inst. of Standards and Technology, Gaithersburg, 2005), `http://webbook.nist.gov/chemistry`

[12] W. Martin, A. Musgrove, S. Kotochigova, and J. Sansonetti, eds., *Ground Levels and Ionization Energies for the Neutral Atoms*, NIST Standard Reference Database No. 111 (Natl. Inst. of Standards and Technology, Gaithersburg, 2010), `http://www.nist.gov/pml/data/ion_energy.cfm`

[13] J. Desclaux, Atomic Data and Nuclear Data Tables **12**, 331 (1973)

[14] D. Sokolovski, Z. Felfli, S. Y. Ovchinnikov, J. H. Macek, and A. Z. Msezane, Phys. Rev. A **76**, 012705 (2007)

[15] C. W. Walter, N. D. Gibson, Y. G. Li, D. J. Matyas, R. M. Alton, S. E. Lou, R. L. F. III, D. Hanstorp, L. Pan, and D. R. Beck, Phys. Rev. A **84**, 032514 (2011)

[16] L. Visscher and K. G. Dyall, Atomic Data and Nuclear Data Tables **67**, 207 (1997). See also the expanded online tables at `http://www.chem.vu.nl/~visscher/FiniteNuclei/FiniteNuclei.htm`

[17] V. T. Davis, J. Thompson, and A. Covington, Nucl. Instrum. Methods Phys. Res. B **241**, 118 (2005)

[18] K. C. Chartkunchand, V. T. Davis, S. S. Duvvuri, Z. A. McCormick, J. S. Thompson, P. P. Wiewior, and A. Covington, Bull. Am. Phys. Soc. **54**, 172 (2009), `http://meetings.aps.org/link/BAPS.2009.DAMOP.Y1.45`

[19] J. Chevary and S. Vosko, J. Phys. B **27**, 657 (1994)